Controllability of structural brain networks and the waxing and waning of negative affect in daily life

McGowan, A.L.[1], Parkes, L.[2], He, X.[2,3], Stanoi, O.[4], Kang, Y.[1], Lomax, S.[1], Mucha, P.J.[5,6], Ochsner, K.N.[3], Falk, E.B.[1,7,8], Bassett, D.S.[2,9,10,11,12,13], & Lydon-Staley, D.M.[1,2,14*]

[1]Annenberg School for Communication, University of Pennsylvania, Philadelphia, PA

[2]Department of Bioengineering, School of Engineering and Applied Science, University of Pennsylvania, Philadelphia, PA, USA

[3]Department of Psychology, School of Humanities and Social Sciences, University of Science and Technology of China, Hefei, P.R. China

[4]Department of Psychology, Columbia University, New York City, NY, USA

[5]Department of Mathematics, University of North Carolina, Chapel Hill, North Carolina, USA

[6]Department of Applied Physical Sciences, University of North Carolina, Chapel Hill, North Carolina, USA

[7]Department of Psychology, University of Pennsylvania, Philadelphia, PA, USA

[8]Marketing Department, Wharton School, University of Pennsylvania, PA, USA

[9]Department of Physics & Astronomy, College of Arts and Sciences, University of Pennsylvania, Philadelphia, PA, USA

[10]Department of Electrical & Systems Engineering, School of Engineering and Applied Science, University of Pennsylvania, Philadelphia, PA, USA

[11]Department of Neurology, Perelman School of Medicine, University of Pennsylvania, Philadelphia, PA, USA

[12]Department of Psychiatry, Perelman School of Medicine, University of Pennsylvania, Philadelphia, PA, USA

[13]Santa Fe Institute, Santa Fe, NM, USA

[14]Leonard Davis Institute of Health Economics, University of Pennsylvania, Philadelphia, PA, USA

*Corresponding author: David M. Lydon-Staley, 3620 Walnut St, Annenberg School for Communication, University of Pennsylvania, Philadelphia, PA 19104 USA. Email: david.lydonstaley@asc.upenn.edu

Abstract

The waxing and waning of negative affect in daily life is normative, reflecting an adaptive capacity to respond flexibly to changing circumstances. Here, we provide insight into facets of brain structure that may enable negative affect variability in daily life. We use diffusion spectrum imaging data from 95 young adults (M_{age} = 20.19 years, SD_{age} = 1.80; 56 women) to construct structural connectivity networks that map white matter fiber connections between 200 cortical and 14 sub-cortical regions. We apply network control theory to these structural networks to estimate the degree to which each brain region's pattern of structural connectivity facilitates the spread of activity to other brain systems (i.e., the region's average controllability). We examine how the average controllability of functional brain systems relates to negative affect variability, computed by taking the standard deviation of negative affect self-reports collected via smartphone-based experience-sampling twice per day over 28 days as participants went about their daily lives. We find that high average controllability of the cingulo-insular system is associated with increased negative affect variability. Our results highlight the role brain structure plays in affective dynamics as observed in the context of daily life.

Keywords: affect variability, average controllability, depression, ecological momentary assessment, network control theory, cingulo-insular system

Controllability of structural brain networks and the waxing and waning of negative affect in daily life

Our lives are given meaning and color by our capacity to experience continuous and dynamically evolving affective responses. The dynamic nature of these experiences (Hollenstein, 2015; Kuppens & Verduyn, 2017) has been documented in behavioral studies that densely sample self-reports of emotion in daily life (Eid & Diener, 1999; Frijda, 1986). These data show that affective variability is normative and is indicative of a capacity to respond flexibly to changing conditions (Brose et al., 2015; Kuppens et al., 2010; Merz & Roesch, 2011). Yet, there are important between-person differences in affect variability. At the extreme, individuals with depression report greater variability in negative affect relative to those without depression (Koval et al., 2013; Lamers et al., 2018; Peeters et al., 2006; Wichers et al., 2010), and greater variability predicts future affect disorder onset and episode recurrence (Houben et al., 2015; Ong & Ram, 2017; Panaite et al., 2020; Wichers et al., 2010).

Between-person differences in affect variability likely stem from multiple sources and may be indicative of the individual, the context in which they are embedded, or the person-context system as a whole (Koffer & Ram, 2015). Here, we focus on the association between brain structure and negative affect variability. The brain can be conceived of as a network of neuronal ensembles or regions (nodes) interlinked by anatomical wires (edges) in a complex and patterned architecture. This connective structure supports the dynamics of neural activity as the brain transitions through functional brain states, traversing a path in a dynamic state-space landscape (Gu et al., 2018; Figure 1). The trajectory of these brain state transitions is modulated by both external and internal perturbations (Bassett & Khambhati, 2017). The ease with which these internal perturbations – driven by activity in individual brain regions – modulate the brain's

trajectory depends on the strength and pattern of structural connections associated with that region (Wu-Yan et al., 2018).

To this end, some individuals may have structural brain network architectures that more easily facilitate changes in brain state trajectories than others, and as a consequence, they may show greater negative affect variability. In particular, we hypothesize that individuals with functional brain systems encompassing cingulate and fronto-insular regions that can more readily drive the brain into different states will exhibit greater negative affect variability. Our hypothesis stems from the fact that this cingulo-insular functional system facilitates access to cognitive control resources (e.g., attention, working memory) that coordinate behavioral responses appropriate to meet the demands of situations (e.g., studying; Menon, 2015; Uddin, 2015). This functional system facilitates access to cognitive control by engaging the frontoparietal system while suppressing default mode system activity (Bonnelle et al., 2012; Sridharan et al., 2008). Thus, by communicating with a distributed network of brain regions to coordinate behavior, this cingulo-insular system is essential to humans' ability to respond adaptively to changes in the environment. Indeed, disruptions in this system are often associated with psychopathology (Hamilton et al., 2013; Liu et al., 2010; Manoliu et al., 2014). Given the cingulo-insular system's role in recruiting other brain systems to facilitate changes in behavior, it is plausible that individuals with systems exhibiting a pattern of structural connectivity that facilitates the spread of activity from this system to other systems of the brain, and with the ability to drive the brain into different states, will show greater negative affect variability.

To test this hypothesis, we used diffusion spectrum imaging data to construct structural connectivity networks that map white matter fiber connections between 200 cortical and 14 sub-cortical regions and applied network control theory, a computational tool originating in the

engineering sciences, to these structural connections (Gu et al., 2015; Karrer et al., 2020). Using network control theory, we modeled the activity of all 214 brain regions using a linear model of dynamics. Specifically, within this framework, regional activity is simulated at each timepoint from a combination of regions' prior activity, the structural connectivity between regions, and external control input (energy delivered over time by the model). We used this model to compute the average controllability of each brain region, which predicts the extent to which each brain region can distribute activity to other regions of the brain to drive the brain into easily reachable states with little input energy. Next, we tested the associations between average controllability of the cingulo-insular system and negative affect variability. We hypothesized that participants with high average controllability of this functional brain system would also have high negative affect variability.

Results

Following well-established methods (Eid & Diener, 1999), we operationalized negative affect variability by taking the intraindividual standard deviation of up to 56 reports (2 per day for 28 days) of current negative affect in 95 (M_{age} = 20.19, SD_{age} = 1.80; 56 women) participants (see Methods for greater detail on participant characteristics). Participants with higher negative affect variability showed a greater range in their negative affect across time relative to participants with lower negative affect variability (Figure 2).

Average controllability of the cingulo-insular system is positively associated with negative affect variability

To determine the extent to which average controllability of the cingulo-insular system is associated with between-person differences in the variability of their self-reported negative affect, we constructed structural connectivity networks from diffusion spectrum imaging data in

the same 95 participants and computed the average controllability of all nodes in the brain for each participant (Figure 1). We took the mean average controllability of nodes within each of the 17 functional systems (Schaefer et al., 2018; Yeo et al., 2011), including the cingulo-insular system, to create system-level average controllability indices. We ran multilevel models to assess the association between average controllability, running separate models for the mean average controllability within each of 17 systems and negative affect variability captured using up to 56 self-reports collected over 28 days (outcome). We controlled for multiple comparisons given our examination of 17 systems using the Benjamini-Hochberg (1995) false discovery rate control.

We provide descriptive statistics and correlations of the variables used in the analyses in Supplemental Table 1. We found that average controllability of the cingulo-insular system (labeled Salience/Ventral Attention A in the Yeo et al., 2011 atlas; nodes included in this functional system are listed in Supplemental Table 2 and associations between these nodes and neurosynth meta-analysis maps are listed in Supplemental Table 3) was positively associated with greater negative affect variability ($b = 9.57$, $p = 0.01$, $q = 0.03$, Cohen's $d = 0.57$; see Supplemental Table 4, Figure 3). Notably, this association was observed when controlling for covariates, including total brain volume, in-scanner motion, and average negative affect. We included average negative affect to ensure the association was specific to variability and not confounded with average negative affect (Eid & Diener, 1999), given that higher average self-reported negative affect was positively associated with negative affect variability ($b = 0.13$, $p = 0.004$, Cohen's $d = 0.65$, see Supplemental Table 4).

To determine the specificity of the association between average controllability of the cingulo-insular system and negative affect variability, we ran multilevel models to assess the association between average controllability and average negative affect, computed as each

individual's mean negative affect across the 56, twice-daily reports. We found no associations between average controllability and average negative affect (*p's* ≥ 0.11). We additionally examined the extent to which our results were specific to average controllability by computing the average strength and clustering coefficient (two commonly used network indices) of the 17 functional brain systems. No associations between negative affect variability and these additional network measures reached statistical significance (see Supplemental Analyses).

Average controllability of the cingulo-insular system promotes normative negative affect variability

In follow-up analyses, we tested the extent to which the observed association between average controllability of the cingulo-insular network reflects normative variation in negative affect variability versus variability that may place individuals at risk for psychopathology. In line with previous work (Chan et al., 2016; Kashdan & Rottenberg, 2010; Waugh et al., 2011), a multilevel Poisson regression revealed that greater negative affect variability related to the presence of more depressive symptoms as measured by the Center for Epidemiological Studies-Depression Scale (CESD; $b = 0.09$, $p = 0.01$, Supplemental Figure 1). However, there was little evidence that average controllability of the cingulo-insular system was statistically significantly associated with depressive symptoms ($b = 0.37$, $p = 0.09$, $d = 0.22$), indicating that negative affect variability was unlikely to mediate the association between controllability of this functional system and depressive symptoms. Finally, when depressive symptoms were included as a covariate in a regression model testing the association between controllability of the cingulo-insular system and negative affect variability, average controllability of the cingulo-insular system remained associated with negative affect variability ($b = 8.42$, $p = 0.03$, Cohen's $d = 0.50$; see Supplemental Table 5).

Discussion

The nature and variability of our affective states are essential ingredients of health and well-being. Here, we sought to explore the structural organization of functional brain systems underlying between-person differences in the extent to which negative affect fluctuates during daily life. Addressing this issue is important because between-person differences in the variability of self-reported negative affect have been associated with depression (Koval et al., 2013; Lamers et al., 2018; Peeters et al., 2006; Wichers et al., 2010). To gain insight into the biological correlates of negative affect variability, we tested the hypothesis that individuals with cingulo-insular systems that have greater ability to facilitate the spread of activity to other brain systems (i.e., average controllability) will show greater negative affect variability in daily life. In line with this hypothesis, we found that average controllability of the cingulo-insular system is positively associated with greater negative affect variability.

The association between average controllability and negative affect variability was specific to the cingulo-insular system. This suggests that this functional system may serve as a key control point in structural brain networks subserving affect dynamics in daily life. Such an interpretation is consistent with the cingulo-insular system's unique role as a system that facilitates behavioral responses to detected events by signaling the engagement and suppression of other brain systems (Menon, 2015; Uddin, 2015). Due to having structural brain network architectures that facilitate the spread of activity from the cingulo-insular network to other systems, individuals with cingulo-insular systems with high average controllability may be more capable of changing their behavior when salient events are detected, which in turn manifests as greater negative affect variability when these changes in behavior are recorded over extended periods of time.

An additional finding of interest is that average controllability of the salience system was unrelated to daily-life average negative affect. This result indicates that having a cingulo-insular system with a pattern of structural connectivity that facilitates the spread of activity to other brain systems is implicated in experiencing greater variability in changing affective states rather than simply experiencing an overall greater intensity of negative affect. This specificity further speaks to the cingulo-insular system's role in affect dynamics. Notably, the ability of the cingulo-insular network to engage with other systems of the brain to promote behavior change is often highlighted as a boon to promote cognitive, affective, and behavioral flexibility (Chen et al., 2016; Lydon-Staley et al., 2019). The current findings suggest that brain network structures that facilitate an especially strong influence of the cingulo-insular system on other brain systems promotes flexibility in affect.

Importantly, follow-up analyses confirm previous work indicating that excessive negative affect variability is associated with greater symptoms of depression (Waugh et al., 2011). However, there was little evidence that this excessive variability, better conceptualized as affective lability (Harvey et al., 1989) and emotion dysregulation, was associated with average controllability of the cingulo-insular system. Instead, average controllability of the cingulo-insular system was associated with normative variation in negative affect variability, in line with the systems role in cognitive and affective flexibility (Lydon-Staley et al., 2019).

In sum, we find that between-person differences in the ease with which the cingulo-insular system can drive the brain into different states is associated with between-person differences in negative affect variability as observed in daily life. These findings provide insight into the role of brain structure in everyday affective experiences and provide additional support for the cingulo-insular system as a key functional brain system involved in affective dynamics.

Methods

We used data from the Social and Health Impact of Network Effects (SHINE) study, a larger study designed to provide insight into health behaviors and social interactions among young adults. All research was conducted in accordance with the Institutional Review Board (IRB) at the University of Pennsylvania and Columbia University, in addition to the Army Research Office. All data and code used in the manuscript are available at http://osf.io/gkahy/. The source code for the average controllability calculation is available at http://github.com/nangongwubu/Network-Controllability-Diagnostics.

Participants and Procedure

Recruitment materials advertised a study titled "Social Health Impact of Network Effects Study (SHINE)" to undergraduate students who were members of on-campus social groups across two universities, University of Pennsylvania and Columbia University. The study was advertised through flyers, university websites, and email communication. To reach campus groups, researchers contacted group leaders as points of contact and further employed a snowball sampling approach, such that participating students could share recruitment information with their peers who were members of on-campus social clubs or sports teams. Of 1024 individuals learning about the study and contacting the study team, 925 individuals were recruited into the study and invited to complete an initial consent form. These participants were asked for their consent to complete an online survey assessing functional Magnetic Resonance Imaging (fMRI) eligibility and an hour-long baseline survey. Participants who completed the consent form and agreed to take part in the study (n=583; 63.03% of invited participants) completed an fMRI screening form and a baseline survey.

Following the baseline survey, participants meeting fMRI inclusion criteria and agreeing to participate in the next part of the study (*n*=112) were randomized into three conditions as part of a larger investigation unrelated to the current report: control (*n*=39), mindfulness (*n*=38), and perspective-taking (*n*=35). Participants attended a laboratory session that included surveys, an MRI session, and instructions for an ecological momentary assessment (EMA) and intervention (EMI) protocol designed to reduce alcohol use (findings are robust to controlling for intervention condition and, as such, we present the most parsimonious models without condition throughout this paper). The day following the laboratory session, participants began a 28-day ecological momentary assessment and protocol. The EMA and EMI was completed by 108 participants from 10 groups in the following conditions: control (*n*=37), mindfulness (*n*=37), and perspective-taking (*n*=34). Participants also completed 6-month and 12-month follow-up online surveys. Participants received up to $105 for participating in the study. Participants received a $20 Amazon gift card for completing the online baseline survey, $50 cash for completing the laboratory session, and a $55 Amazon gift card for answering at least 70% of ecological momentary assessments. We focus on the baseline survey, the MRI session, and the ecological momentary assessment and refer readers to http://osf.io/gkahy/ for greater detail about the rest of the protocol.

The participants reported on in this manuscript (see Supplemental Figure 2 for a CONSORT flow diagram of enrollment and retention through the study periods) comprise 95 young adults aged 18 to 28 years old (*M* = 20.19, *SD* = 1.80, 56 women). Participants identified as Asian (30.5%); Black or African American (2.1%); Latino/a (5.3%); white (52.6%); and as multiple categories: white, American Indian or Alaska Native (2.1%); white, Asian (3.2%); white, Asian,

Native Hawaiian or other Pacific Islander (1.1%); and white, Latino/a (3.2%). Data collection began in February 2019 and ended in April 2020.

MRI data acquisition, preprocessing, and modeling. Imaging data were acquired on 3-Tesla Siemens Trio scanners equipped with a 64-channel head coil. The DWI data were preprocessed and reconstructed through QSIprep v 0.8.0 (Cieslak et al., 2020). Briefly, the data was first denoised and bias corrected, and then underwent susceptibility distortion correction, motion and eddy current correction via FSL 6.0, and coregistered to T1 space. We also warped both the Schaefer atlas (Schaefer et al., 2018) and the Harvard Oxford subcortical atlas (Smith et al., 2004) into individual T1 space to subdivide the brain into 200 cortical and 14 subcortical regions. Then, the preprocessed DWI data was reconstructed using generalized Q-sampling Imaging (Yeh et al., 2010) in DSI-Studio (http://dsi-studio.labsolver.org). Deterministic tractography (Yeh et al., 2013) was performed until 5×10^6 streamlines were reconstructed, yielding individual structural networks with brain regions as nodes and the number of streamlines connecting each brain region pair as weighted edges. Preprocessing was performed using QSIPrep 0.8.0, which is based on Nipype 1.4.2 (Gorgolewski et al., 2011, 2018; RRID:SCR_002502).

Anatomical data preprocessing. The T1-weighted (T1w) image was corrected for intensity non-uniformity (INU) using N4BiasFieldCorrection (Tustison et al., 2010), and used as T1w-reference throughout the workflow. The T1w-reference was then skull-stripped using antsBrainExtraction.sh (ANTs 2.3.1), using OASIS as the target template. Spatial normalization to the ICBM 152 Nonlinear Asymmetrical template version 2009c (Fonov et al., 2009) was performed through nonlinear registration with antsRegistration (ANTs 2.3.1, RRID:SCR_004757; Avants et al., 2008), using brain-extracted versions of both T1w volume

and template. Brain tissue segmentation of cerebrospinal fluid (CSF), white-matter (WM) and gray-matter (GM) was performed on the brain-extracted T1w using FAST (FSL 6.0.3:b862cdd5, RRID:SCR_002823, Zhang et al., 2001).

Diffusion data preprocessing. MP-PCA denoising as implemented in MRtrix3's dwidenoise (Veraart et al., 2016) was applied with a 5- voxel window. After MP-PCA, Gibbs unringing was performed using MRtrix3's mrdegibbs (Kellner et al., 2016). Following unringing, B1 field inhomogeneity was corrected using dwibiascorrect from MRtrix3 with the N4 algorithm (Tustison et al., 2010). After B1 bias correction, the mean intensity of the DWI series was adjusted so all the mean intensity of the b=0 images matched across each separate DWI scanning sequence. FSL (version 6.0.3:b862cdd5)'s eddy was used for head motion correction and Eddy current correction (Andersson & Sotiropoulos, 2016). Eddy was configured with a q-space smoothing factor of 10, a total of 5 iterations, and 1000 voxels used to estimate hyperparameters. A linear first level model and a linear second level model were used to characterize Eddy current-related spatial distortion. q-space coordinates were forcefully assigned to shells. Field offset was attempted to be separated from subject movement. Shells were aligned post-eddy. Eddy's outlier replacement was run (Andersson & Sotiropoulos, 2016). Data were grouped by slice, only including values from slices determined to contain at least 250 intracerebral voxels. Groups deviating by more than 4 standard deviations from the prediction had their data replaced with imputed values. Fieldmaps were collected with reversed phase-encode blips, resulting in pairs of images with distortions going in opposite directions. Here, a b=0 fieldmap image with reversed phase encoding direction was used along with b=0 images extracted from the DWI scans. From these pairs, the susceptibility-induced off-resonance field was estimated using a method similar to that described in(Andersson et al., 2003). The fieldmaps

were ultimately incorporated into the Eddy current and head motion correction interpolation. Final interpolation was performed using the jac method.

Several confounding time-series were calculated based on the preprocessed DWI: framewise displacement (FD) using the implementation in Nipype (following the definitions by Power et al., 2014). The head-motion estimates calculated in the correction step were also placed within the corresponding confounds file. Slicewise cross correlation was also calculated. The DWI time-series were resampled to ACPC, generating a preprocessed DWI run in ACPC space with 1.7 mm isotropic voxels. Many internal operations of QSIPrep use Nilearn 0.7.0 (Abraham et al., 2014; RRID:SCR_001362) and Dipy (Contributors et al., 2014).

Ecological momentary assessment. On the day after the laboratory session, participants began a 28-day ecological momentary assessment period. Each day, participants answered two signal-contingent surveys per day. A morning survey was sent at 8:00 AM and an evening survey was sent at 6:00 PM. The surveys assessed affect, alcohol consumption, and a range of other variables (see http://osf.io/gkahy/ for codebook).

Measures

We used participants' reports of demographic information from the baseline surveys, their ratings of negative affect during the 28-day experience-sampling period, and diffusion spectrum imaging (DSI) to create structural brain networks.

Negative affect. Negative affect was measured every morning and evening in response to the question "How negative do you feel right now?" on a scale of 1 (not at all) to 100 (extremely) in increments of 1. Out of a possible total of 5376 negative affect reports, 4982 (92.7%) were available. Participants completed 18 to 56 affect reports (M = 52.44, SD = 6.56) across the experience-sampling period.

Average negative affect. Average negative affect was calculated using the intraindividual mean across each participant's day's negative affect reports (M = 37.38, SD = 14.29).

Negative affect variability. Negative affect variability was calculated using the intraindividual standard deviation across each participant's day's negative affect reports (M = 17.88, SD = 6.44).

Depression. Depression was measured using the 10-item version of the Center for Epidemiological Studies-Depression Scale (CESD-10; Radloff, 1977). All items included four response categories indicating the frequency of depressive symptoms *during the past week* on a four-point scale of 0 (rarely or none of the time, less than 1 day), 1 (some or a little of the time, 1-2 days), 2 (occasionally or a moderate amount of the time, 3-4 days), or 3 (most or all of the time, 5-7 days). The scoring of positive items is reversed and the possible range of scores is 0 to 30 (*Median* = 9.78, SD = 5), with higher scores indicating the presence of more depressive symptoms.

Average controllability. From the DWI data, we constructed anatomical brain networks by subdividing the brain into 214 regions using the Schaefer atlas for 200 cortical regions and the Harvard Oxford atlas for 14 subcortical regions. In these anatomical connectivity matrices, brain regions are defined as nodes, and a link between two nodes represents the number of streamlines connecting them, normalized for density (Sotiropoulos & Zalesky, 2019).

We drew on Network Control Theory to assess the extent to which large-scale brain networks exert control over other large-scale brain networks. Controllability of a dynamical system describes the possibility of driving the current state of a system to a desired target state via external control input (Tang & Bassett, 2018). Such an approach allows us to gain better insight into the relationship between brain structure and brain dynamics. Here, we focus on

average controllability, which quantifies each region's capacity to leverage the brain's underlying structural connectivity to distribute activity throughout the brain to guide changes between easily reachable states (Gu et al., 2015). Networks with high average controllability are more influential in the control of network dynamics, driving the system into different states with little effort (i.e., input energy). The relationship of the mathematical formulation of network control to brain networks is discussed in more detail in Gu *et al.* (2015). To ensure system stability, each participant's structural connectivity matrix was normalized by dividing each element by the largest absolute eigenvalue of the matrix plus one (Karrer et al., 2020). Following normalization, average controllability was calculated for each node. Next, rank-based inverse normal transformations were applied to each node across participants to ensure normality (McCaw et al., 2020). Finally, we calculated the mean average controllability over nodes within each of 17 functional brain systems (Schaefer et al., 2018; Yeo et al., 2011). These system-averaged estimates of average controllability were taken into subsequent analyses of between-person differences (see below for further details).

Statistical Analysis

We tested the extent to which negative affect variability was associated with average controllability of 17 functional brain systems (Yeo et al., 2011) using 17 separate multilevel models, one for each system. We used multilevel models to account for the nested nature of the data (95 participants nested in 10 groups). We included *average negative affect, total brain volume*, and *in-scanner motion* as covariates. In all models, we specified a random intercept for *group* (as participants were nested in social groups). All analyses used the nlme package in R (Pinheiro, 2009).

Acknowledgements

Research was sponsored by the Army Research Office and was accomplished under Grant Number W911NF-18-1-0244. D.M.L. and A.L.M. acknowledge support from the National Institute on Drug Abuse (K01 DA047417) and the Brain & Behavior Research Foundation. D.S.B. acknowledges support from the John D. and Catherine T. MacArthur Foundation, the Swartz Foundation, the Paul G. Allen Family Foundation, the Alfred P. Sloan Foundation and the NSF (PHY-1554488; IIS-1926757). D.S.B. and L. P. acknowledge support from the National Institute of Mental Health (R01MH113550), and L.P. acknowledges support from the 2020 NARSAD Young Investigator Grant from the Brain & Behavior Research Foundation. The views and conclusions contained in this document are those of the authors and should not be interpreted as representing the official policies, either expressed or implied, of the Army Research Office or the U.S. Government. The U.S. Government is authorized to reproduce and distribute reprints for Government purposes notwithstanding any copyright notation herein.

Citation Diversity Statement

Recent work in several fields of science has identified a bias in citation practices such that papers from women and other minority scholars are under-cited relative to the number of such papers in the field (Bertolero et al., 2020; Caplar et al., 2017; Chakravartty et al., 2018; Dion et al., 2018; Dworkin et al., 2020; Fulvio et al., 2020; Maliniak et al., 2013; Mitchell et al., 2013; Wang et al., 2020). Here we sought to proactively consider choosing references that reflect the diversity of the field in thought, form of contribution, gender, race, ethnicity, and other factors. First, we obtained the predicted gender of the first and last author of each reference by using databases that store the probability of a first name being carried by a woman (Dworkin et al., 2020; Zhou et

al., 2020). By this measure (and excluding self-citations to the first and last authors of our current paper), our references contain 13.33% woman(first)/woman(last), 15.61% man/woman, 15.0% woman/man, and 56.05% man/man. This method is limited in that a) names, pronouns, and social media profiles used to construct the databases may not, in every case, be indicative of gender identity and b) it cannot account for intersex, non-binary, or transgender people. We look forward to future work that could help us to better understand how to support equitable practices in science.

References

Abraham, A., Pedregosa, F., Eickenberg, M., Gervais, P., Mueller, A., Kossaifi, J., Gramfort, A., Thirion, B., & Varoquaux, G. (2014). Machine learning for neuroimaging with scikit-learn. *Frontiers in Neuroinformatics*, *8*, 14.

Andersson, J. L., Skare, S., & Ashburner, J. (2003). How to correct susceptibility distortions in spin-echo echo-planar images: Application to diffusion tensor imaging. *Neuroimage*, *20*(2), 870–888.

Andersson, J. L., & Sotiropoulos, S. N. (2016). An integrated approach to correction for off-resonance effects and subject movement in diffusion MR imaging. *Neuroimage*, *125*, 1063–1078.

Avants, B. B., Epstein, C. L., Grossman, M., & Gee, J. C. (2008). Symmetric diffeomorphic image registration with cross-correlation: Evaluating automated labeling of elderly and neurodegenerative brain. *Medical Image Analysis*, *12*(1), 26–41.

Bassett, D. S., & Khambhati, A. N. (2017). A network engineering perspective on probing and perturbing cognition with neurofeedback. *Annals of the New York Academy of Sciences*, *1396*(1), 126.

Benjamini, Y., & Hochberg, Y. (1995). Controlling the false discovery rate: A practical and powerful approach to multiple testing. *Journal of the Royal Statistical Society: Series B (Methodological)*, *57*(1), 289–300.

Bertolero, M. A., Dworkin, J. D., David, S. U., Lloreda, C. L., Srivastava, P., Stiso, J., Zhou, D., Dzirasa, K., Fair, D. A., & Kaczkurkin, A. N. (2020). Racial and ethnic imbalance in neuroscience reference lists and intersections with gender. *BioRxiv*.

Bonnelle, V., Ham, T. E., Leech, R., Kinnunen, K. M., Mehta, M. A., Greenwood, R. J., & Sharp, D. J. (2012). Salience network integrity predicts default mode network function after traumatic brain injury. *Proceedings of the National Academy of Sciences*, *109*(12), 4690–4695.

Brose, A., Schmiedek, F., Koval, P., & Kuppens, P. (2015). Emotional inertia contributes to depressive symptoms beyond perseverative thinking. *Cognition and Emotion*, *29*(3), 527–538.

Caplar, N., Tacchella, S., & Birrer, S. (2017). Quantitative evaluation of gender bias in astronomical publications from citation counts. *Nature Astronomy*, *1*(6), 1–5.

Chakravartty, P., Kuo, R., Grubbs, V., & McIlwain, C. (2018). # CommunicationSoWhite. *Journal of Communication*, *68*(2), 254–266.

Chan, D. K., Zhang, X., Fung, H. H., & Hagger, M. S. (2016). Affect, affective variability, and physical health: Results from a population-based investigation in China. *International Journal of Behavioral Medicine*, *23*(4), 438–446.

Chen, T., Cai, W., Ryali, S., Supekar, K., & Menon, V. (2016). Distinct global brain dynamics and spatiotemporal organization of the salience network. *PLoS Biology*, *14*(6), e1002469.

Cieslak, M., Cook, P. A., He, X., Yeh, F.-C., Dhollander, T., Adebimpe, A., Aguirre, G. K., Bassett, D. S., Betzel, R. F., & Bourque, J. (2020). QSIPrep: An integrative platform for preprocessing and reconstructing diffusion MRI. *BioRxiv*.

Contributors, D., Garyfallidis, E., Brett, M., Amirbekian, B. B., Rokem, A., van der Walt, S., Descoteaux, M., & Nimmo-Smith, I. (2014). Dipy, a library for the analysis of diffusion MRI data. *Frontiers in Neuroinformatics*, *8*, 8.

Dion, M. L., Sumner, J. L., & Mitchell, S. M. (2018). Gendered citation patterns across political science and social science methodology fields. *Political Analysis*, *26*(3), 312–327.

Dworkin, J. D., Linn, K. A., Teich, E. G., Zurn, P., Shinohara, R. T., & Bassett, D. S. (2020). The extent and drivers of gender imbalance in neuroscience reference lists. *ArXiv Preprint ArXiv:2001.01002*.

Eid, M., & Diener, E. (1999). Intraindividual variability in affect: Reliability, validity, and personality correlates. *Journal of Personality and Social Psychology*, *76*(4), 662. https://doi.org/10.1037/0022-3514.76.4.662

Fonov, V. S., Evans, A. C., McKinstry, R. C., Almli, C. R., & Collins, D. L. (2009). Unbiased nonlinear average age-appropriate brain templates from birth to adulthood. *NeuroImage*, *47*, S102.

Frijda, N. H. (1986). *The emotions*. Cambridge University Press.

Fulvio, J. M., Akinnola, I., & Postle, B. R. (2020). Gender (im) balance in citation practices in cognitive neuroscience. *Journal of Cognitive Neuroscience*, 1–5.

Gorgolewski, K. J., Burns, C. D., Madison, C., Clark, D., Halchenko, Y. O., Waskom, M. L., & Ghosh, S. S. (2011). Nipype: A flexible, lightweight and extensible neuroimaging data processing framework in python. *Frontiers in Neuroinformatics*, *5*, 13.

Gorgolewski, K. J., Esteban, O., Markiewicz, C. J., Ziegler, E., Ellis, D. G., Notter, M. P., Jarecka, D., Johnson, H., Burns, C., & Manhaes-Savio, A. (2018). Nipype. *Software, Zenodo*.

Gu, S., Cieslak, M., Baird, B., Muldoon, S. F., Grafton, S. T., Pasqualetti, F., & Bassett, D. S. (2018). The energy landscape of neurophysiological activity implicit in brain network structure. *Scientific Reports*, *8*(1), 1–15.

Gu, S., Pasqualetti, F., Cieslak, M., Telesford, Q. K., Yu, A. B., Kahn, A. E., Medaglia, J. D., Vettel, J. M., Miller, M. B., Grafton, S. T., & Bassett, D. S. (2015). Controllability of structural brain networks. *Nature Communications*, *6*(1), 8414. https://doi.org/10.1038/ncomms9414

Hamilton, J. P., Chen, M. C., & Gotlib, I. H. (2013). Neural systems approaches to understanding major depressive disorder: An intrinsic functional organization perspective. *Neurobiology of Disease*, *52*, 4–11. https://doi.org/10.1016/j.nbd.2012.01.015

Harvey, P. D., Greenberg, B. R., & Serper, M. R. (1989). The affective lability scales: Development, reliability, and validity. *Journal of Clinical Psychology*, *45*(5), 786–793.

Hollenstein, T. (2015). This time, it's real: Affective flexibility, time scales, feedback loops, and the regulation of emotion. *Emotion Review*, *7*(4), 308–315.

Houben, M., Van Den Noortgate, W., & Kuppens, P. (2015). The relation between short-term emotion dynamics and psychological well-being: A meta-analysis. *Psychological Bulletin*, *141*(4), 901.

Karrer, T. M., Kim, J. Z., Stiso, J., Kahn, A. E., Pasqualetti, F., Habel, U., & Bassett, D. S. (2020). A practical guide to methodological considerations in the controllability of structural brain networks. *Journal of Neural Engineering*, *17*(2), 026031.

Kashdan, T. B., & Rottenberg, J. (2010). Psychological flexibility as a fundamental aspect of health. *Clinical Psychology Review*, *30*(7), 865–878. https://doi.org/10.1016/j.cpr.2010.03.001

Kellner, E., Dhital, B., Kiselev, V. G., & Reisert, M. (2016). Gibbs-ringing artifact removal based on local subvoxel-shifts. *Magnetic Resonance in Medicine*, *76*(5), 1574–1581.

Koffer, R., & Ram, N. (2015). Intraindividual variability. *The Encyclopedia of Adulthood and Aging*, 1–7.

Koval, P., Pe, M. L., Meers, K., & Kuppens, P. (2013). Affect dynamics in relation to depressive symptoms: Variable, unstable or inert? *Emotion*, *13*(6), 1132. https://doi.org/10.1037/a0033579

Kuppens, P., Allen, N. B., & Sheeber, L. B. (2010). Emotional inertia and psychological maladjustment. *Psychological Science*, *21*(7), 984–991.

Kuppens, P., & Verduyn, P. (2017). Emotion dynamics. *Current Opinion in Psychology*, *17*, 22–26.

Lamers, F., Swendsen, J., Cui, L., Husky, M., Johns, J., Zipunnikov, V., & Merikangas, K. R. (2018). Mood reactivity and affective dynamics in mood and anxiety disorders. *Journal of Abnormal Psychology*, *127*(7), 659. https://doi.org/10.1037/abn0000378

Liu, Z., Xu, C., Xu, Y., Wang, Y., Zhao, B., Lv, Y., Cao, X., Zhang, K., & Du, C. (2010). Decreased regional homogeneity in insula and cerebellum: A resting-state fMRI study in patients with major depression and subjects at high risk for major depression. *Psychiatry Research: Neuroimaging*, *182*(3), 211–215. https://doi.org/10.1016/j.pscychresns.2010.03.004

Lydon-Staley, D. M., Kuehner, C., Zamoscik, V., Huffziger, S., Kirsch, P., & Bassett, D. S. (2019). Repetitive negative thinking in daily life and functional connectivity among default mode, fronto-parietal, and salience networks. *Translational Psychiatry*, *9*(1), 1–12.

Maliniak, D., Powers, R., & Walter, B. F. (2013). The gender citation gap in international relations. *International Organization*, *67*(4), 889–922.

Manoliu, A., Meng, C., Brandl, F., Doll, A., Tahmasian, M., Scherr, M., Schwerthöffer, D., Zimmer, C., Förstl, H., & Bäuml, J. (2014). Insular dysfunction within the salience network is associated with severity of symptoms and aberrant inter-network connectivity in major depressive disorder. *Frontiers in Human Neuroscience*, *7*, 930.

McCaw, Z. R., Lane, J. M., Saxena, R., Redline, S., & Lin, X. (2020). Operating characteristics of the rank-based inverse normal transformation for quantitative trait analysis in genome-wide association studies. *Biometrics*, *76*(4), 1262–1272.

Menon, V. (2015). *Salience Network: Brain Mapping: An Encyclopedic Reference*. Elsevier.

Merz, E. L., & Roesch, S. C. (2011). Modeling trait and state variation using multilevel factor analysis with PANAS daily diary data. *Journal of Research in Personality*, *45*(1), 2–9. https://doi.org/10.1016/j.jrp.2010.11.003

Mitchell, S. M., Lange, S., & Brus, H. (2013). Gendered citation patterns in international relations journals. *International Studies Perspectives*, *14*(4), 485–492.

Ong, A. D., & Ram, N. (2017). Fragile and Enduring Positive Affect: Implications for Adaptive Aging. *Gerontology*, *63*(3), 263–270. https://doi.org/10.1159/000453357

Panaite, V., Rottenberg, J., & Bylsma, L. M. (2020). Daily Affective Dynamics Predict Depression Symptom Trajectories Among Adults with Major and Minor Depression. *Affective Science*, *1*(3), 186–198. https://doi.org/10.1007/s42761-020-00014-w

Parkes, L., Moore, T. M., Calkins, M. E., Cieslak, M., Roalf, D. R., Wolf, D. H., Gur, R. C., Gur, R. E., Satterthwaite, T. D., & Bassett, D. S. (2021). Network controllability in transmodal cortex predicts positive psychosis spectrum symptoms. *Biological Psychiatry*. https://doi.org/10.1016/j.biopsych.2021.03.016

Peeters, F., Berkhof, J., Delespaul, P., Rottenberg, J., & Nicolson, N. A. (2006). Diurnal mood variation in major depressive disorder. *Emotion*, *6*(3), 383.

Pinheiro, J. (2009). nlme: Linear and nonlinear mixed effects models. R package version 3.1-96. *Http://Cran. r-Project. Org/Web/Packages/Nlme/*.

Power, J. D., Mitra, A., Laumann, T. O., Snyder, A. Z., Schlaggar, B. L., & Petersen, S. E. (2014). Methods to detect, characterize, and remove motion artifact in resting state fMRI. *Neuroimage*, *84*, 320–341.

Radloff, L. S. (1977). The CES-D scale: A self-report depression scale for research in the general population. *Applied Psychological Measurement*, *1*(3), 385–401.

Schaefer, A., Kong, R., Gordon, E. M., Laumann, T. O., Zuo, X.-N., Holmes, A. J., Eickhoff, S. B., & Yeo, B. T. (2018). Local-global parcellation of the human cerebral cortex from intrinsic functional connectivity MRI. *Cerebral Cortex*, *28*(9), 3095–3114.

Smith, S. M., Jenkinson, M., Woolrich, M. W., Beckmann, C. F., Behrens, T. E., Johansen-Berg, H., Bannister, P. R., De Luca, M., Drobnjak, I., & Flitney, D. E. (2004). Advances in functional and structural MR image analysis and implementation as FSL. *Neuroimage*, *23*, S208–S219.

Sotiropoulos, S. N., & Zalesky, A. (2019). Building connectomes using diffusion MRI: Why, how and but. *NMR in Biomedicine*, *32*(4), e3752.

Sridharan, D., Levitin, D. J., & Menon, V. (2008). A critical role for the right fronto-insular cortex in switching between central-executive and default-mode networks. *Proceedings of the National Academy of Sciences*, *105*(34), 12569–12574.

Tang, E., & Bassett, D. S. (2018). Colloquium: Control of dynamics in brain networks. *Reviews of Modern Physics*, *90*(3), 031003.

Tang, E., Giusti, C., Baum, G. L., Gu, S., Pollock, E., Kahn, A. E., Roalf, D. R., Moore, T. M., Ruparel, K., & Gur, R. C. (2017). Developmental increases in white matter network controllability support a growing diversity of brain dynamics. *Nature Communications*, *8*(1), 1–16.

Tustison, N. J., Avants, B. B., Cook, P. A., Zheng, Y., Egan, A., Yushkevich, P. A., & Gee, J. C. (2010). N4ITK: Improved N3 bias correction. *IEEE Transactions on Medical Imaging*, *29*(6), 1310–1320.

Uddin, L. Q. (2015). Salience processing and insular cortical function and dysfunction. *Nature Reviews Neuroscience*, *16*(1), 55–61.

Veraart, J., Novikov, D. S., Christiaens, D., Ades-Aron, B., Sijbers, J., & Fieremans, E. (2016). Denoising of diffusion MRI using random matrix theory. *Neuroimage*, *142*, 394–406.

Wang, X., Dworkin, J., Zhou, D., Stiso, J., Falk, E., Zurn, P., Bassett, D., & Lydon-Staley, D. M. (2020). *Gendered Citation Practices in the Field of Communication*.

Waugh, C. E., Thompson, R. J., & Gotlib, I. H. (2011). Flexible emotional responsiveness in trait resilience. *Emotion*, *11*(5), 1059.

Wichers, M., Peeters, F., Geschwind, N., Jacobs, N., Simons, C. J. P., Derom, C., Thiery, E., Delespaul, P. H., & Van Os, J. (2010). Unveiling patterns of affective responses in daily life may improve outcome prediction in depression: A momentary assessment study. *Journal of Affective Disorders*, *124*(1–2), 191–195.

Wu-Yan, E., Betzel, R. F., Tang, E., Gu, S., Pasqualetti, F., & Bassett, D. S. (2018). Benchmarking measures of network controllability on canonical graph models. *Journal of Nonlinear Science*, 1–39.

Yeh, F.-C., Verstynen, T. D., Wang, Y., Fernández-Miranda, J. C., & Tseng, W.-Y. I. (2013). Deterministic diffusion fiber tracking improved by quantitative anisotropy. *PloS One*, *8*(11), e80713.

Yeh, F.-C., Wedeen, V. J., & Tseng, W.-Y. I. (2010). Generalized q-sampling imaging. *IEEE Transactions on Medical Imaging*, *29*(9), 1626–1635.

Yeo, B. T. T., Krienen, F. M., Sepulcre, J., Sabuncu, M. R., Lashkari, D., Hollinshead, M., Roffman, J. L., Smoller, J. W., Zöllei, L., Polimeni, J. R., Fischl, B., Liu, H., & Buckner, R. L. (2011). The organization of the human cerebral cortex estimated by intrinsic functional connectivity. *Journal of Neurophysiology*, *106*(3), 1125–1165. https://doi.org/10.1152/jn.00338.2011

Zhang, Y., Brady, M., & Smith, S. (2001). Segmentation of brain MR images through a hidden Markov random field model and the expectation-maximization algorithm. *IEEE Transactions on Medical Imaging*, *20*(1), 45–57.

Zhou, D., Cornblath, E. J., Stiso, J., Teich, E. G., Dworkin, J. D., Blevins, A. S., & Bassett, D. S. (2020). Gender diversity statement and code notebook v1. 0. 2020. *URL Https://Doi. Org/10.5281/Zenodo*, *3672110*.

Figure Captions

Figure 1. Construction of average controllability indices. **A.** Participants (*n*=95) underwent diffusion spectrum imaging. **B.** The resulting data underwent tractography to map white matter fiber streamline connections between 214 cortical and subcortical regions. **C.** The resulting structural brain networks consist of nodes (brain regions) connected by edges, links between nodes representing the number of streamlines connecting them, normalized for density (Sotiropoulos & Zalesky, 2019). **D.** Structural brain networks are analyzed in a network control framework (Gu et al., 2015; Manoliu et al., 2014; Parkes et al., 2021) to compute the structural support that network offers for moving the brain to easy-to-reach states following control input. Figures adapted from Parkes et al. (2021) and Tang et al. (2017).

Figure 2. Between-person differences in negative affect variability. **A.** Participants provided up to 56 reports (two reports per day for 28 days) of their negative affect on their smartphones as they went about their daily lives in an ecological momentary assessment protocol. The time series of negative affect reports of two participants is shown in panels **B** and **C**. Both participants exhibit similar mean (*M*) values of negative affect across the 56 reports, as indicated by the black dashed line. However, the participant in panel **C** shows greater variability in their negative affect around their mean affect, relative to the participant in panel **B** as highlighted in grey. This greater negative affect variability is captured by the intraindividual standard deviation of the negative affect time series (*SD*).

Figure 3. Greater average controllability of the cingulo-insular system is associated with greater negative affect variability. **A.** Multilevel models indicate that the strongest association, indicated by Cohen's *d*, between negative affect variability and average controllability was observed in the

cingulo-insular system (labelled Salience/Ventral Attention A in Yeo et al., 2011). The association between average controllability and negative affect variability was only significant in the cingulo-insular system. **B.** Participants with higher average controllability values (x-axis; average of rank-based inverse normal transformed within each network within each individual) exhibited higher negative affect variability (y-axis) in their daily lives. Note that the association between average controllability and negative affect variability remains significant when the potential outlier on the left is removed.

Figure 1.

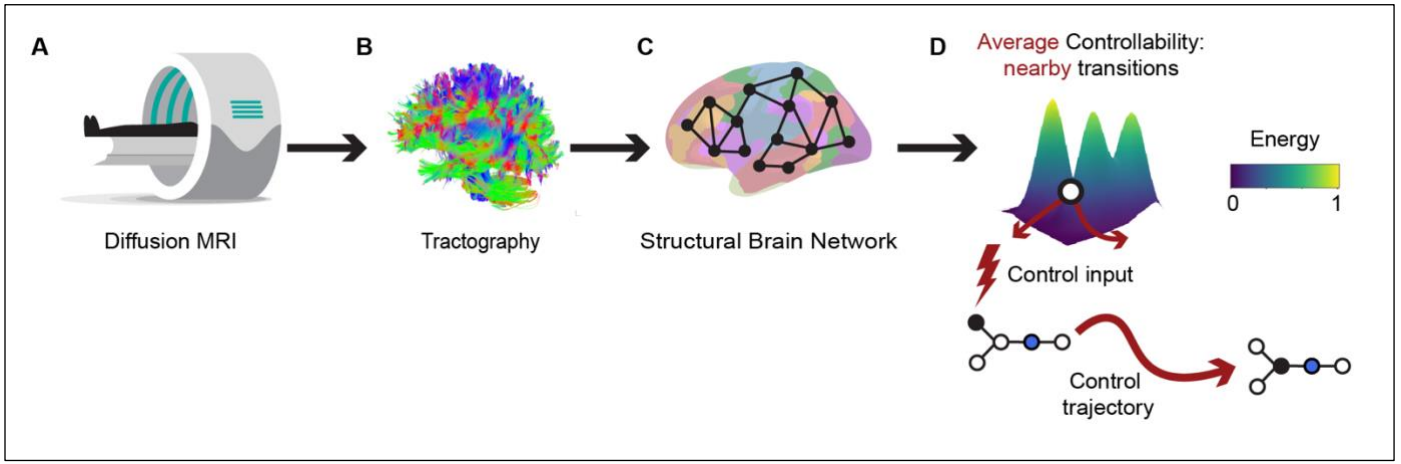
A
B
C
D
Average Controllability:
nearby transitions
Energy
0
1
Diffusion MRI
Tractography
Structural Brain Network
Control input
Control
trajectory

Figure 2.

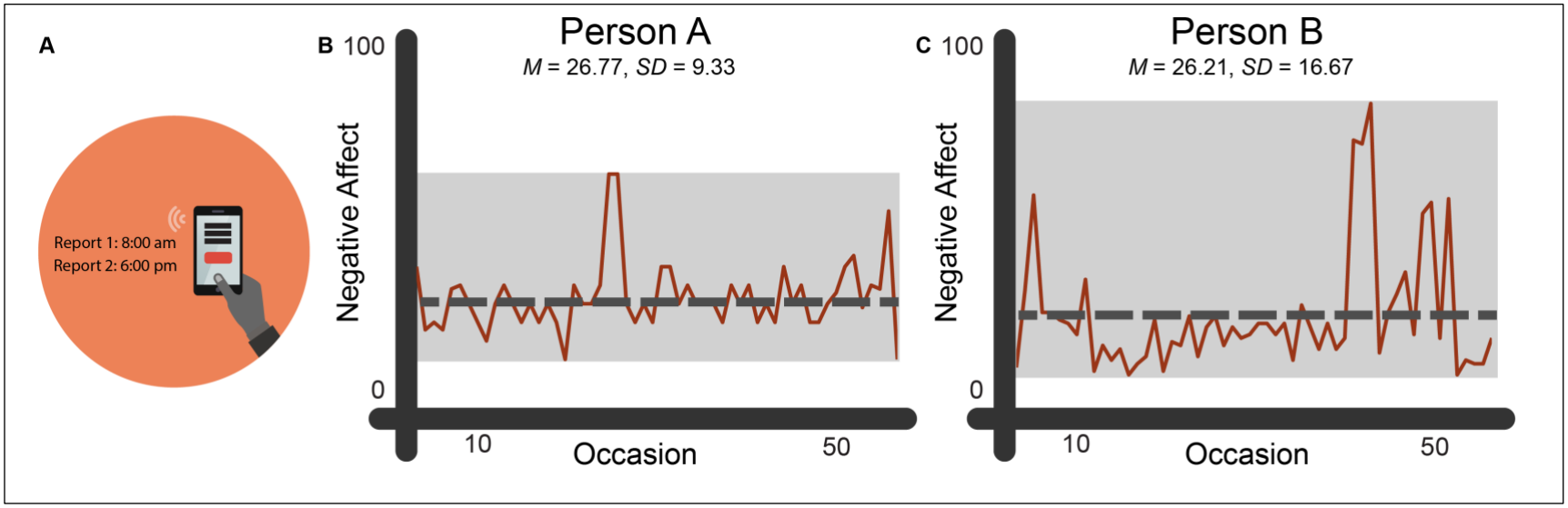
A
Report 1: 8:00 am
Report 2: 6:00 pm
B
Person A
M = 26.77, SD = 9.33
100
Negative Affect
0
10
Occasion
50
C
Person B
M = 26.21, SD = 16.67
100
Negative Affect
0
10
Occasion
50

Figure 3.

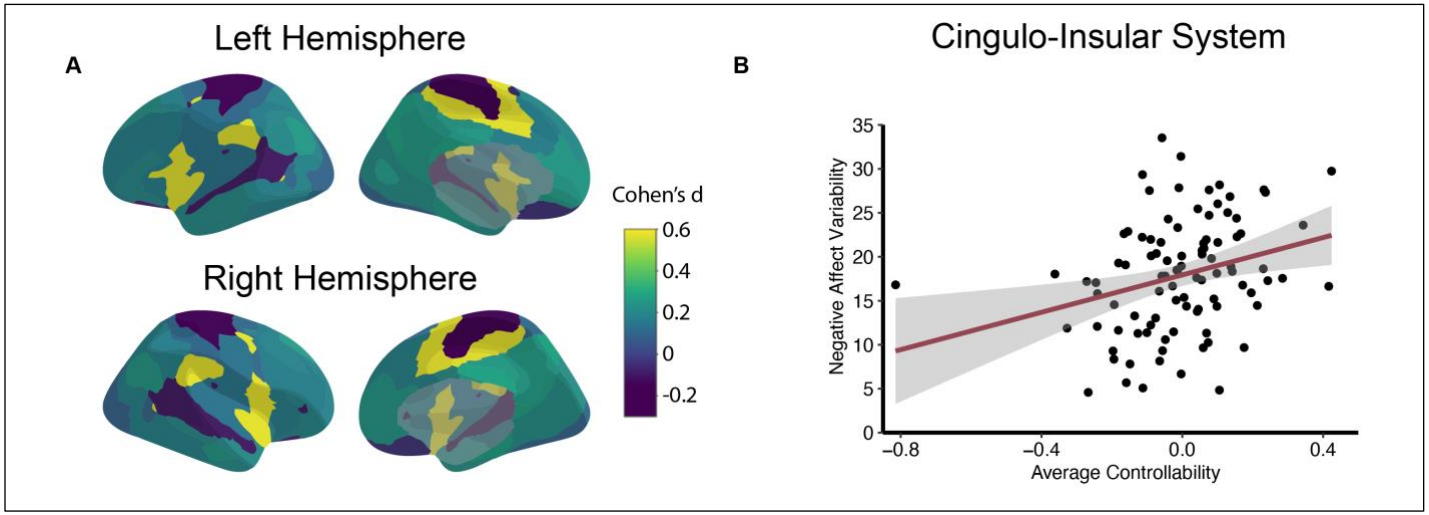
A
Left Hemisphere
Right Hemisphere
Cohen's d
0.6
0.4
0.2
0
-0.2
B
Cingulo-Insular System
Negative Affect Variability
35
30
25
20
15
10
5
0
−0.8
−0.4
0.0
0.4
Average Controllability